

# Planar quantum squeezing and atom interferometry

Q. Y. He

*ARC Centre of Excellence for Quantum-Atom Optics,  
Centre for Atom Optics and Ultrafast Spectroscopy,  
Swinburne University of Technology, Melbourne 3122, Australia*

Shi-Guo Peng

*Department of Physics, Tsinghua University, Beijing 100084, China*

P. D. Drummond\*

*ARC Centre of Excellence for Quantum-Atom Optics,  
Centre for Atom Optics and Ultrafast Spectroscopy,  
Swinburne University of Technology, Melbourne 3122, Australia*

M. D. Reid†

*ARC Centre of Excellence for Quantum-Atom Optics,  
Centre for Atom Optics and Ultrafast Spectroscopy,  
Swinburne University of Technology, Melbourne 3122, Australia*

We obtain a lower bound on the sum of two orthogonal spin component variances in a plane. This gives a novel planar uncertainty relation which holds even when the Heisenberg relation is not useful. We investigate the asymptotic, large  $J$  limit, and derive the properties of the planar quantum squeezed states that saturate this uncertainty relation. These states extend the concept of spin squeezing to any two conjugate spin directions. We show that planar quantum squeezing can be achieved experimentally as the ground state of a Bose-Einstein condensate in two coupled potential wells with a critical attractive interaction. These states reduce interferometric phase noise at all phase angles simultaneously. This is useful for one-shot interferometric phase-measurements where the measured phase is completely unknown. Our results can also be used to derive entanglement criteria for multiple spins  $J$  at separated sites, with applications in quantum information.

## I. INTRODUCTION

Heisenberg's famous uncertainty relation for angular momentum takes the well-known product form  $\Delta J_X \Delta J_Y \geq |\langle \hat{J}_Z \rangle|/2$ . If  $\langle \hat{J}_Z \rangle = 0$ , as in a singlet state, the Heisenberg relation becomes trivial: it only constrains the spin variances to positive values. Nevertheless, there are still fundamental limits to these uncertainties, which are directly related to quantum limits on interferometric phase measurements [1–5], together with problems like macroscopic entanglement [6–9], Bohm's Einstein-Podolsky-Rosen (EPR) paradox [10] and steering [11–14].

Reduction of quantum noise in one spin component - or single-axis squeezing - is a valuable tool for enhancing the sensitivity of interferometers and atomic clocks [1, 2]. It has been recently implemented for ultra-cold atomic Bose-Einstein condensate (BEC) interferometers [3–5]. This type of quantum noise reduction reduces the measurement noise near some predetermined phase. However, if the phase is completely unknown prior to measurement, then it is not known which phase quadrature should be in a squeezed state.

In this paper we demonstrate that spin operators permit another type of quantum squeezing that we call planar quantum squeezing (PQS), which simultaneously reduces the quantum noise of two orthogonal spin projections below the standard quantum limit of  $J/2$ , while increasing the noise in a third dimension. This allows the prospect of improved phase measurements at any phase-angle. PQS states that reduce fluctuations everywhere in a plane have potential utility in 'one-shot' phase measurements, where iterative or repeated measurement strategies cannot be utilized.

Planar quantum squeezing is related to a planar uncertainty relation, true for any quantum state. This has the form of a lower bound on the planar spin variance sum [7, 15],

$$\Delta^2 \mathbf{J}_{\parallel} \geq C_J. \quad (1.1)$$

Here  $\mathbf{J}_{\parallel}$  is the spin projection parallel to a plane, so in the  $X - Y$  plane,  $\Delta^2 \mathbf{J}_{\parallel} \equiv \Delta^2 J_X + \Delta^2 J_Y$ , and  $C_J$  is the minimum of the uncertainty sum for quantum states with fixed spin  $J$ . While values of  $C_J$  for  $J = 1/2$  [15] and  $J = 1$  [7] were known previously, we calculate  $C_J$  for arbitrary spin quantum number  $J$ . We show that the  $C_J$  uncertainty principle has a fractional exponent behavior, with  $C_J \sim J^{2/3}$ , and that states saturating this uncertainty condition have variances with the same fractional power law exponents in two orthogonal directions. These also have a mean spin vector in the direction of

\* pdrummond@swin.edu.au

† mdreid@swin.edu.au

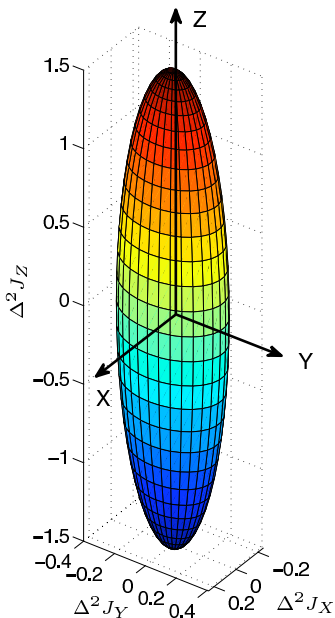


Figure 1. (Color online) Three-dimensional plot of uncertainties for planar quantum squeezing. The figure corresponds to 100 atoms ( $J = 50$ ) in the ground-state of a double-well Bose-Einstein condensate with critical attractive interaction. Spin variances are reduced in both axes parallel to the  $X - Y$  plane, with a maximum variance reduction in the mean spin direction  $X$ . The variance must increase perpendicular to the squeezing plane, along the  $Z$  axis.

greatest variance reduction. The variance perpendicular to the squeezing plane is increased, with  $\Delta^2 J_{\perp} \sim J^{4/3}$ . The overall three-dimensional variance has an ellipsoidal shape, graphed in Fig. 1. We show that the ground state of a two-mode Bose-Einstein condensate (BEC) with attractive interactions gives the maximum possible PQS, making this an important candidate for interferometric measurements.

As well as allowing improved interferometric phase measurements, planar uncertainty relations are useful for the detection of non-classical behavior in mesoscopic systems with large total spin  $J$ . The general form of the corresponding two-spin Local Uncertainty Relation (LUR) criterion to detect entanglement among  $N$  sites of spin  $J$  particles is

$$\Delta^2 \mathbf{J}_{\parallel}^{total} < NC_J, \quad (1.2)$$

where  $J^{total}$  represents the collective spin operator, and the particular case of  $N = 2$  has been considered by Hofmann and Takeuchi [7] as a criterion for entanglement between two sites. Larger  $N$  values signify multipartite entanglement. Experiments involving measurements in two spin directions [16] have employed a similar inequality to detect genuine multipartite entanglement in four qubit states [17].

We extend this microscopic analysis to mesoscopic spins of *arbitrary*  $J$ , and hence show that equation (1.2) is a multipartite entanglement criterion for  $N$  sites. This

entanglement signature is valid in the mesoscopic limit of large  $J$ , and applies regardless of the third component, which may not be readily measurable.

## II. PLANAR UNCERTAINTY RELATIONS

Our first task is to find the lower bound  $C_J$  of the planar uncertainty relation equation (1.1). We consider states of fixed spin dimensionality  $J$ . The most general pure quantum state of this type has dimension  $d = 2J + 1$ . Expressed in the  $J_Z$  basis, this state is:

$$|\psi\rangle = \frac{1}{\sqrt{n}} \sum_{m=-J}^J R_m e^{-i\phi_m} |J, m\rangle \quad (2.1)$$

Here  $R_m, \phi_m$  ( $m = -J, \dots, J$ ) are real numbers indicating amplitude and phase respectively, and the normalization coefficient is  $n = \sum_{m=-J}^J R_m^2$ .

### A. Uncertainty Minimization

To obtain a lower bound on the variance sum we minimize the uncertainty over all possible expansion coefficients, using:

$$\Delta^2 \mathbf{J}_{\parallel} \equiv \left\langle \left| \hat{\mathbf{J}}_{\parallel} \right|^2 \right\rangle - \left| \langle \hat{\mathbf{J}}_{\parallel} \rangle \right|^2. \quad (2.2)$$

Due to spherical symmetry, it is enough to consider the uncertainty relation in the  $X - Y$  plane. We can choose axes in the  $X - Y$  plane so that  $\langle \hat{J}_Y \rangle = 0$ , with no loss of generality. We calculate the expectation values in the  $Z$  basis. We find that the squared projections are

$$\left\langle \left| \hat{\mathbf{J}}_{\parallel} \right|^2 \right\rangle = -\frac{1}{4} + \frac{1}{n} \sum_{m=-J}^J R_m^2 \left[ \tilde{J}^2 - m^2 \right], \quad (2.3)$$

where we have defined  $\tilde{J} \equiv J + 1/2$ . On maximizing the magnitude with respect to the phase variable, and introducing  $M \equiv m + 1/2$ ,  $M_{\pm} = M \pm 1/2$ , we find that the mean projections satisfy:

$$\langle \hat{J}_X \rangle = \pm \frac{1}{n} \sum_{M=-\tilde{J}}^{\tilde{J}} R_{M+} R_{M-} \sqrt{\tilde{J}^2 - M^2}. \quad (2.4)$$

Using these equations, we can numerically obtain the value of  $C_J$  for any spin  $J$ , by using nonlinear optimization techniques (we used the quasi-Newton method implemented via the Mathematica 8.0 *FindMinimum* function[18]) to search for the minimum value of equation (2.2) given any possible coefficients.

The results for selected values of  $J$  are tabulated in Table I, and  $C_J/J$  is graphed in Fig. 2 by dots.

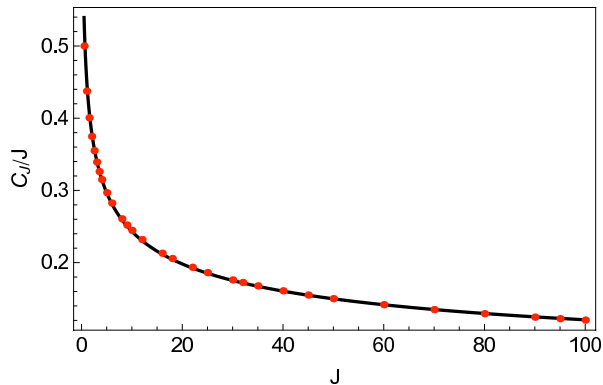


Figure 2. (Color online) Graph of planar uncertainty relation bound. The figure plots the lower bound to the planar uncertainty relation, normalized by  $J$ , the standard quantum limit. Note that  $C_J/J$  shows a decrease with increasing  $J$ . Discrete points are calculated numerically, while the solid line is the analytic approximation  $C_J^{(a)}$ .

$J$	$C_J$
$\frac{1}{2}$	1/4
1	7/16
$\frac{3}{2}$	0.6009
2	0.7496
$\frac{5}{2}$	0.8877
3	1.018
$\frac{7}{2}$	1.142
4	1.260
5	1.484
6	1.695
7	1.894
10	2.445
20	3.984
50	7.503

Table I. Lower bound  $C_J$  of the planar uncertainty equation. Numerical results for equation (1.1) are tabulated as a function of spin  $J$ .

### B. Asymptotic $C_J$ values:

We wish to obtain the asymptotic, large  $J$  limit of the planar uncertainty principle using an integral approximation. The mean spin projections for any quantum state

are:

$$\begin{aligned} \langle \hat{J}_X \rangle &= \frac{1}{n} \sum_{m=-J}^J \{ \sqrt{(J-m)(J+m+1)} \\ &\quad \times \cos(\phi_m - \phi_{m+1}) R_m R_{m+1} \}, \\ \langle \hat{J}_Y \rangle &= \frac{1}{n} \sum_{m=-J}^J \{ \sqrt{(J-m)(J+m+1)} \\ &\quad \times \sin(\phi_m - \phi_{m+1}) R_m R_{m+1} \}, \\ \langle \hat{J}_Z \rangle &= 0. \end{aligned} \quad (2.5)$$

For  $J \rightarrow \infty$  we replace the summation over  $2J+1$  discrete values of  $m$  by an integral over a continuous range of  $(-1, 1)$ . We define  $\tilde{J} = J + 1/2$ , and introduce scaled variables of  $x = m/\tilde{J}$  and  $r(x) = R_m \sqrt{\tilde{J}}$ , so that the normalization integral becomes:

$$n = \sum_{m=-J}^J R_m^2 \approx \int_{-1}^1 r^2(x) dx. \quad (2.6)$$

For the mean squared spin vector, taking equation (2.3) in the limit of  $J \rightarrow \infty$  one obtains

$$\left\langle \left| \hat{\mathbf{J}}_{\parallel} \right|^2 \right\rangle \approx -\frac{1}{4} + \frac{1}{n} \int_{-1}^1 r^2(x) J^2(x) dx, \quad (2.7)$$

where  $J(x) \equiv \tilde{J} \sqrt{1-x^2}$ .

For the mean value term  $\langle \hat{\mathbf{J}}_{\parallel} \rangle$  in equation (2.4), we also replace summations by integrals in the limit of  $J \rightarrow \infty$  and define a slightly modified variable  $x = M/\tilde{J}$ . Next, using a Taylor expansion, we obtain:

$$r(x \pm \frac{1}{2\tilde{J}}) = r(x) \pm \frac{1}{2\tilde{J}} \frac{dr(x)}{dx} + \frac{1}{8\tilde{J}^2} \frac{d^2r(x)}{dx^2} + O\left(\frac{1}{\tilde{J}^3}\right). \quad (2.8)$$

After integrating by parts, and defining  $r'(x) = dr(x)/dx$ , this can be expressed as a variational calculus problem. We minimize  $V[r] \equiv \Delta^2 \mathbf{J}_{\parallel}$  as a function of  $r(x)$ , where

$$\begin{aligned} V[r] &\approx -\frac{1}{4} + \int_{-1}^1 r^2(x) \frac{J^2(x)}{n} dx \\ &\quad - \left[ \int_{-1}^1 \left( r^2(x) - \frac{(r'(x))^2}{2\tilde{J}^2} + \frac{xr(x)r'(x)}{4J^2(x)} \right) \frac{J(x) dx}{n} \right]^2. \end{aligned} \quad (2.9)$$

Due to the symmetry of the integrand around  $x = 0$ , the minimum function  $r(x)$  must have a reflection symmetry with a maximum at  $x = 0$ . In the large  $J$  limit we can assume a relatively narrow Gaussian solution of variance  $\sigma \ll 1$ , where  $\sigma \sim J^{-\nu}$ ,  $\nu$  is still undetermined, and:

$$r(x) = \left(\frac{1}{2\pi\sigma}\right)^{1/4} e^{-x^2/4\sigma}. \quad (2.10)$$

With this choice, we can extend the integration limits to  $x = \pm\infty$  to leading order in  $1/J$ . This means that  $n = 1$ ,

and on expanding the integrand one finds that:

$$V[r] \approx \tilde{J}^2 \int_{-\infty}^{\infty} r^2(x) [1 - x^2] dx \quad (2.11)$$

$$- \left[ \tilde{J} \int_{-\infty}^{\infty} r^2(x) \left(1 - \frac{x^2}{8\sigma^2\tilde{J}^2}\right) \sqrt{1 - x^2} dx \right]^2.$$

Next, we expand the variational integral, retaining leading terms only. We use the results that:

$$\int_{-\infty}^{\infty} r^2(x) x^2 dx = \sigma$$

$$\int_{-\infty}^{\infty} r^2(x) x^4 dx = 3\sigma^2$$

$$\int_{-\infty}^{\infty} r^2(x) \sqrt{1 - x^2} dx = 1 - \frac{\sigma}{2} - \frac{3\sigma^2}{8} + \dots, \quad (2.12)$$

giving a corresponding asymptotic estimate for  $C_J$  of

$$V[r] \approx \frac{1}{4\sigma} [1 + 2\sigma^3 J^2] \dots \quad (2.13)$$

Applying variational calculus so that  $dV/d\sigma = 0$ , and solving in the limit of large  $J$ , we find that  $\sigma = (2J)^{-2/3}$ . This means that:

$$\lim_{J \rightarrow \infty} C_J \approx 3(2J)^{2/3}/8 = 0.595275J^{2/3}. \quad (2.14)$$

Using this asymptotic form, and numerically fitting the tabulated results with a series in  $J^{1/3}$ , we obtain the following analytic approximation to  $C_J$ :

$$C_J^{(a)} \simeq 0.595275J^{2/3} - 0.1663J^{1/3} + 0.0267. \quad (2.15)$$

This is given in Fig. 2 by the solid curve, in good agreement with our numerical results: within 1% for  $J \geq 5$ .

### III. CHARACTERIZATION OF THE MINIMUM VARIANCE STATE

We now wish to characterize the properties of the state that minimizes a planar variance sum. The main difference can be seen if one considers that not all the states that minimize the Heisenberg product have planar squeezing. For example, the state with  $\langle \hat{J}_Z \rangle = -J$  is an eigenstate of the spin projection in the  $Z$  direction. This gives a minimum variance (zero) in one direction, but cannot minimize the variance sum. It is not a planar squeezed state, since the orthogonal variances are not reduced below the standard quantum limit.

#### A. Optimum planar squeezed state:

We wish to analyze the detailed asymptotic properties of the planar quantum squeezed state that saturates the uncertainty principle. We consider states of fixed spin dimensionality  $J$ , and calculate the mean value of  $\langle \hat{\mathbf{J}} \rangle$

in the  $J_Z$  basis as in equation (2.5). As previously, we choose axes with squeezing in the  $X-Y$  plane and  $\langle \hat{J}_Y \rangle = 0$ . By selecting the phase as  $\phi_m = 0$ , we get a minimum planar variance, and a non-vanishing mean value in  $\langle \hat{J}_X \rangle$ . This is a generic property of planar squeezed minimum variance states, which always have a spin vector with a finite mean amplitude in the plane of minimum variance.

The value of the spin variance in each direction in the plane still needs to be calculated, in order to define the properties of the planar squeezed state. We assume a symmetric amplitude distribution with  $R_m = R_{-m}$ , so that  $\langle \hat{J}_Z \rangle = 0$ . The mean values are then given as in equation (2.4), by:

$$\langle \hat{J}_X \rangle = \frac{1}{n} \sum_{M=-\tilde{J}}^{M=\tilde{J}} R_{M+} R_{M-} \sqrt{\tilde{J}^2 - M^2},$$

$$\langle \hat{J}_Y \rangle = \langle \hat{J}_Z \rangle = 0. \quad (3.1)$$

Introducing  $J_+ = J + 1$ ,  $m_+ = m + 1$ , we find the squared spin projections and correlations are:

$$\langle \hat{J}_X^2 \rangle = \frac{1}{2n} \left\{ \sum_{m=-J}^J [J^2 - m^2 + J] R_m^2 \right. \quad (3.2)$$

$$\left. + \sum_{m=-J}^{J-2} \sqrt{[J_+^2 - m_+^2]} [J^2 - m_+^2] R_m R_{m+2} \right\},$$

$$\langle \hat{J}_Y^2 \rangle = \frac{1}{2n} \left\{ \sum_{m=-J}^J [J^2 - m^2 + J] R_m^2 \right. \quad (3.3)$$

$$\left. - \sum_{m=-J}^{J-2} \sqrt{[J_+^2 - m_+^2]} [J^2 - m_+^2] R_m R_{m+2} \right\},$$

$$\langle \hat{J}_Z^2 \rangle = \frac{1}{n} \sum_{m=-J}^J m^2 R_m^2, \quad (3.4)$$

$$\langle \hat{J}_X \hat{J}_Y \rangle = \langle \hat{J}_X \hat{J}_Z \rangle = \langle \hat{J}_Z \hat{J}_Y \rangle = 0. \quad (3.5)$$

We now treat the asymptotic, large  $J$  limit using an integral approximation as previously. For the mean value term, on replacing summations by integrals, in the limit of  $J \rightarrow \infty$  and defining  $x = M/\tilde{J}$ ,  $r(x) = R_M \sqrt{\tilde{J}}$  and  $\bar{J}_X = \langle J_X \rangle$  we obtain:

$$\bar{J}_X = \int_{-1}^1 \left( r^2(x) - \frac{(r'(x))^2}{2\tilde{J}^2} + \frac{xr(x)r'(x)}{4J^2(x)} \right) J(x) dx, \quad (3.6)$$

where  $J(x) \equiv \tilde{J}\sqrt{1-x^2}$ . We know that  $\sigma = (2J)^{-2/3}$  to get the minimum variance. To leading order, one finds that:

$$\bar{J}_X = \tilde{J} \int_{-1}^1 r^2(x) \left(1 - \frac{x^2}{8\sigma^2\tilde{J}^2}\right) J(x) dx, \quad (3.7)$$

Next, we expand the variational integral, retaining leading terms only, giving

$$\bar{J}_X \approx \tilde{J} \left[1 - \frac{\sigma}{2} - \frac{3\sigma^2}{8} - \frac{1}{8\sigma^2\tilde{J}^2}\right] \sim J \left[1 - \frac{1}{2(2J)^{2/3}}\right] \quad (3.8)$$

Similarly, on evaluating the square of the z-projection, we find that:

$$\langle \hat{J}_Z^2 \rangle = \tilde{J}^2\sigma + \frac{1}{4} \sim (J^2/2)^{2/3}. \quad (3.9)$$

The sum of planar variances is simple to calculate. Following the techniques given previously, we find that:

$$\langle \hat{J}_X^2 + \hat{J}_Y^2 \rangle = \tilde{J}^2(1 - \sigma) - \frac{1}{2}. \quad (3.10)$$

This means that we carry out a check on the total spin, which is given by the expected result of:

$$\begin{aligned} \langle \hat{J}_X^2 + \hat{J}_Y^2 + \hat{J}_Z^2 \rangle &= \tilde{J}^2 - \frac{1}{4} \\ &= J(J+1). \end{aligned} \quad (3.11)$$

However, the individual planar variances are more complex. Introducing scaled variables of  $x = (m+1)/J = M'J$ , one must use a Taylor expansion so that:

$$\begin{aligned} r(x \pm \frac{1}{J}) &= r(x) \pm \frac{1}{J}r'(x) + \frac{1}{2J^2}r''(x) + O(\frac{1}{J^3}) \\ &= r(x) \mp \frac{x}{2J\sigma}r(x) - \frac{r(x)}{4J^2\sigma} + \frac{x^2r(x)}{8J^2\sigma^2} + O(\frac{1}{J^3}). \end{aligned} \quad (3.12)$$

After carrying out the integrals, we find that the squared projections in the plane are:

$$\begin{aligned} \langle \hat{J}_X^2 \rangle &= J^2 \left[1 - \sigma - \frac{1}{4J^2\sigma} + \frac{1}{J} + \frac{1}{4J^2}\right] \\ \langle \hat{J}_Y^2 \rangle &= \frac{1}{4} \left[\frac{1}{\sigma} - 1\right]. \end{aligned} \quad (3.13)$$

on subtracting the mean values squared, this gives the result that to leading order:

$$\begin{aligned} \Delta^2 J_X &\sim \frac{(2J)^{2/3}}{8}, \\ \Delta^2 J_Y &\sim \frac{(2J)^{2/3}}{4}, \\ \Delta^2 J_Z &\sim (J^2/2)^{2/3}, \end{aligned} \quad (3.14)$$

and hence the Heisenberg uncertainty principle in the  $Z - Y$  plane is obeyed, since:

$$\Delta J_Z \Delta J_Y \sim \frac{J}{2} \geq |\langle \hat{J}_Z \rangle|/2. \quad (3.15)$$

On calculating the mean and variance of each spin component, we find that that the plane of squeezing always includes the mean spin direction  $\langle \hat{\mathbf{J}} \rangle$ . Choosing axes so that this projection is in the  $X$  direction, with planar squeezing in the  $X - Y$  plane, we calculate that:  $\langle \hat{J}_X \rangle \sim J - \frac{1}{2}(J/4)^{1/3}$ ,  $\Delta^2 J_X \sim \frac{1}{8}(2J)^{2/3}$ ,  $\Delta^2 J_Y \sim \frac{1}{4}(2J)^{2/3}$ ,  $\Delta^2 J_Z \sim (J^2/2)^{2/3}$ . Asymptotically this is a Heisenberg limited or 'intelligent' [19] state in the  $Z - Y$  plane since:

$$\Delta J_Y \Delta J_Z \approx \frac{1}{2} |\langle \hat{J}_X \rangle|. \quad (3.16)$$

In summary, the important features of the optimum planar squeezed state are:

- A large spin expectation *parallel* to the plane of squeezing
- Maximum variance reduction in the direction of the mean spin vector
- A smaller variance reduction in the plane of squeezing orthogonal to the mean spin
- Saturation of the  $C_J$  uncertainty relation
- A complementary variance increase in the third dimension
- Heisenberg limited asymptotic uncertainties *perpendicular* to the mean spin vector

## IV. APPLICATIONS OF PLANAR QUANTUM SQUEEZING

### A. Generation of PQS in a BEC

We first wish to consider how to generate these PQS states. While there are many possible strategies, the simplest is to find a physical system whose Hamiltonian equals the variance sum. The ground state of such a Hamiltonian will minimize the variance, hence creating a perfect planar squeezed state. This can be readily achieved in a two-mode Bose-Einstein condensate, which has been experimentally demonstrated to generate spin-squeezing [3, 4]. In the limit of tight confinement and small numbers of atoms, this type of system can be treated using a simple coupled mode effective Hamiltonian, where  $\kappa$  is the inter-well tunneling rate between wells, and  $g$  is the intra-well s-wave interaction between the atoms. The system is depicted schematically in Fig.

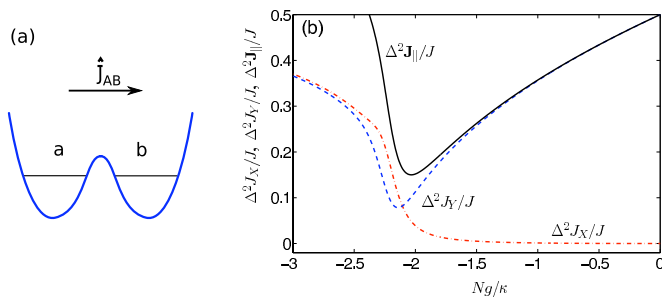


Figure 3. (Color online) (a) Schematic diagram of double-well Bose-Einstein condensate. Shows a schematic double potential well, with corresponding pseudo-spin operator. (b) Spin variances for the ground state of a double-well BEC. Here  $N = 100$  atoms, or  $J = 50$ . The solid line is the total variance, the dashed line is the Y-axis spin projection variance, the dot-dashed line is the X-axis variance in the mean spin direction.

3. We note that the total particle number is conserved, with eigenvalue  $N = 2J$ , where  $J$  is the equivalent effective spin quantum number.

Following standard techniques [22–24], the two-well BEC Hamiltonian can be written in spin language, ignoring conserved terms proportional to  $\hat{N}$  or  $\hat{N}^2$ . We start with a two-mode Hamiltonian in the standard form:

$$\hat{H}/\hbar = \kappa \left[ \hat{a}^\dagger \hat{b} + \hat{b}^\dagger \hat{a} \right] + \frac{g}{2} \left[ \hat{a}^\dagger \hat{a}^\dagger \hat{a} \hat{a} + \hat{b}^\dagger \hat{b}^\dagger \hat{b} \hat{b} \right]. \quad (4.1)$$

Inter-well spin operators have already been measured in this environment, and are defined as:

$$\hat{\mathbf{J}}_{\parallel} = \left( \frac{1}{2} \left[ \hat{a}^\dagger \hat{b} + \hat{a} \hat{b}^\dagger \right], \frac{1}{2i} \left[ \hat{a}^\dagger \hat{b} - \hat{a} \hat{b}^\dagger \right] \right),$$

$$\hat{J}_{\perp} = \left( \hat{a}^\dagger \hat{a} - \hat{b}^\dagger \hat{b} \right) / 2, \quad (4.2)$$

It is convenient to introduce a symmetry breaking vector  $\mathbf{J}_0 = (\kappa/g, 0)$ , which causes tunneling, to give:

$$\hat{H}/\hbar = -g \left| \hat{\mathbf{J}}_{\parallel} - \mathbf{J}_0 \right|^2. \quad (4.3)$$

It is clear from this form of the Hamiltonian that with an attractive coupling so that  $g < 0$ , the ground state will *exactly* minimize the planar variance, provided the tunneling rate  $\kappa$  is adjusted so that  $\langle \hat{\mathbf{J}} \rangle = \mathbf{J}_0$ . Since we have already calculated the optimum mean spin vector, we therefore expect that a planar squeezed state will occur as the ground state of the Hamiltonian for an attractive coupling ( $g < 0$ ), with  $\kappa/|g| = \left| \langle \hat{J}_X \rangle \right| = J - \frac{1}{2} (J/4)^{1/3}$ . The eigenstates of this Hamiltonian can be readily calculated numerically from its matrix form. It is known to have a macroscopic inter-well spatial entanglement [20–22], which is maximized at a critical attractive coupling value [22–24].

A graph of the variances against coupling is shown in Fig. 3b, showing the expected reduction in both variances at a critical value of the coupling. For  $N = 100$ ,

the total planar spin variance reaches its minimum value with a coupling value of  $Ng/\kappa = -2.034 = N/\langle \hat{J}_X \rangle$ , as expected. At the minimum variance, we find numerically that:

$$\Delta^2 \mathbf{J}_{\parallel} = 0.1501 J = C_{50}. \quad (4.4)$$

This is in excellent agreement with equation (2.15), which gives  $C_{50}^{(a)} = 0.1499 J$ . Similar good agreement is obtained for the calculated values of  $\langle \hat{\mathbf{J}}_X \rangle$ ,  $\Delta^2 \mathbf{J}$ , compared with the asymptotic equations (3.8), (3.14), and (3.15) – apart from corrections of order  $1/J^2$ .

In summary, the ground state of a two-well BEC is not only a planar squeezed state: at critical coupling it gives the *exact* solution to the minimum variance. However, while spin-squeezing has been observed experimentally [3–5], indicating that detection at the quantum shot-noise level is technically feasible, existing experiments used a BEC with repulsive interactions. To obtain a PQS state would require an experiment using attractive interactions, as found in  $^{39}\text{K}$ , for example [28]. We finally note that Einstein-Podolsky-Rosen entanglement and macroscopic superpositions for BEC states have been topics of recent interest [22, 25–27]. It is intriguing that the simplest physical route towards generating planar-squeezed states also displays other important physical properties, including macroscopic entanglement [22]. In this case we emphasize that the entanglement is found between the two underlying boson modes which are used to construct the composite spin operators.

## B. Applications to Interferometry

Due to their interactions with magnetic and gravitational fields, cold atomic sensors have been useful for ultra-sensitive magnetometers [29] and gravimeters [30, 31]. In this section, we analyze the possible applications of planar spin squeezing in atom interferometry [32]. In order to improve the performance of this type of sensor it is important to combine both relatively large atom numbers [33] and quantum noise reduction [4, 5]. Consider the effect of the spin mapping to a pair of boson modes which are subsequently passed through a beam splitter (for external degrees of freedom) or microwave rotation (in the case of internal degrees of freedom) [1, 2]. We use the mapping defined in the previous section in equation (4.2), with a planar quantum squeezed input.

Next, we consider the effects of an idealized phase-measurement. This is shown in schematic form in Fig 4. Two bosonic modes  $\hat{a}$ ,  $\hat{b}$  prepared in an entangled PQS state, are passed through phase-shifters and a four-port 50 : 50 beam-splitter. Here  $\phi$  is an unknown phase-shift to be measured, while  $\theta$  is a reference phase-shift. The number difference between the output ports,  $N^+ - N^-$  is measured, and gives information about the unknown phase.

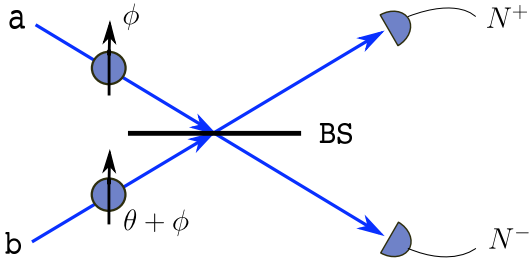


Figure 4. (Color online) Schematic diagram of ideal interferometric measurements. Phase measurements can be reduced in the simplest case to an output measurement of number differences from a beam-splitter, where  $\phi$  is the unknown phase-shift and  $\theta$  is a known reference phase-shift.

After the phase shifters, but before the beam splitter, the collective spin components in the  $X - Y$  plane are:

$$\begin{aligned}\hat{J}_X(\phi) &= \hat{J}_X \cos(\phi - \theta) + \hat{J}_Y \sin(\phi - \theta), \\ \hat{J}_Y(\phi) &= \hat{J}_Y \cos(\phi - \theta) - \hat{J}_X \sin(\phi - \theta).\end{aligned}\quad (4.5)$$

After the beam splitter, we define two output operators as

$$\hat{c}_{\pm} = [\hat{a}e^{i\phi} \pm \hat{b}e^{i\theta}] / \sqrt{2}. \quad (4.6)$$

Calculating the phase-sensitive output number difference,  $\hat{\mathcal{N}} = [\hat{N}^+ - \hat{N}^-]$ , and its derivative in terms of the measured phase, we find that the measured phase uncertainty is:

$$\Delta\phi = \frac{\sqrt{\Delta^2 \mathcal{N}(\phi)}}{|\partial \mathcal{N} / \partial \phi|} \quad (4.7)$$

The phase noise in a single measurement in terms of the initial spin variances, in a state where  $\langle J_X J_Y \rangle = 0$ , is therefore:

$$\Delta\phi = \frac{\sqrt{\Delta^2 J_X \cos^2(\phi - \theta) + \Delta^2 J_Y \sin^2(\phi - \theta)}}{|\bar{J}_Y \cos(\phi - \theta) - \bar{J}_X \sin(\phi - \theta)|}.$$

Clearly, in any phase measurement one must avoid insensitive regimes of the interferometer near the fringe peaks where  $\bar{J}_Y(\phi) = \partial \mathcal{N} / \partial \phi \sim 0$ . We see that the quantum noise in each measurement is bounded above since:

$$\Delta^2 J_X \cos^2(\phi - \theta) + \Delta^2 J_Y \sin^2(\phi - \theta) \leq \Delta^2 \mathbf{J}_{\parallel}. \quad (4.8)$$

This shows clearly that the planar variance is an upper bound to the total quantum noise on the interferometer number difference output. Squeezing this upper bound below the standard quantum limit is vital under conditions where the measured phase is completely unknown. Planar quantum squeezed states therefore can provide useful noise reductions over a large range of unknown phases. In the best case, one can achieve  $\Delta^2 \mathbf{J}_{\parallel} \sim C_J \sim J^{2/3}$ , which leads to a phase uncertainty of:

$$\Delta\phi \propto J^{-2/3}. \quad (4.9)$$

This has the utility of allowing much lower atom numbers and therefore lower atomic density in atom interferometry at a given phase sensitivity. Since the atom density is limited by two-body and three-body losses, this is a very significant practical advantage. To give an example, a PQS interferometer with  $10^6$  atoms has a phase sensitivity of order  $10^{-4}$  in a single phase measurement. To achieve this result with conventional coherent interferometry would require  $10^8$  atoms, which implies 100 times greater density for the same geometry.

## V. PLANAR SQUEEZING ENTANGLEMENT CRITERIA

In earlier works, uncertainty relations have been used extensively for the derivation of criteria to detect entanglement, the EPR paradox and mesoscopic superpositions [7–12, 16, 17, 34–46]. However, neither the Heisenberg [37] nor the related Sorenson-Molmer [39, 44] inequalities can be used to detect the entanglement of a very important subclass of states that have  $\langle \mathbf{J} \rangle = 0$ . This includes the maximally entangled states which are eigenstates of  $J_Z$  having  $\langle \hat{J}_Z \rangle = 0$ . In these cases, that give rise to the classic violations of local realism studied originally by Bell [47, 48], the variance of the remaining spins are still constrained, because no simultaneous eigenstates exist.

It is in this situation our more general two-component uncertainty relation involving both variances is extremely useful [7]. This two-component criterion can also detect the entanglement of the Bell-type maximally entangled states, only requiring the measurement of two orthogonal spin components [7], as well as determining the possible existence of multi-particle genuine entanglement. A further application of the planar uncertainty relation equation (1.1) is that it provides a means of witnessing multipartite entanglement between macroscopic spins.

Hofmann and Takeuchi [7] have proved that any uncertainty relation of the type  $\Delta^2 \mathbf{A} \geq U_A$ , where the system is labelled  $A$  and  $\mathbf{A}$  is a vector of observables for that system, can be used to define a criterion for entanglement. Here the limit  $U$  is generically defined as the absolute minimum of the uncertainty sum for any quantum state. The planar uncertainty equation (1.1) is of this form. If systems  $A$  and  $B$  are separable, then it is always true that

$$\Delta^2 (\mathbf{A} + \mathbf{B}) \geq U_A + U_B. \quad (5.1)$$

The violation of this uncertainty bound is then a proof of entanglement. This result may be generalized to multipartite systems consisting of  $N$  distinct locations, as shown by Toth [8, 9, 40, 49]. Consider  $N$  sites of spin  $J$  particles. Assuming absolute separability, we write the total density matrix  $\hat{\rho}$  as a probabilistic sum of product density matrices  $\hat{\rho}_R^k$  at site  $k$ , occurring with probability

$P_R$ :

$$\hat{\rho} = \sum_R P_R \hat{\rho}_R^1 \hat{\rho}_R^2 \dots \hat{\rho}_R^N. \quad (5.2)$$

Defining collective spin operators as

$$\hat{J}_i^{total} = \sum_{k=1}^N c_{k,i} \hat{J}_i^k, \quad (5.3)$$

where  $c_{k,i} = \pm 1$ , the expression for the sum of the variances is

$$\Delta^2 \mathbf{J}_{\parallel}^{total} \geq \sum_R P_R \sum_{k=1}^N (\Delta^2 \mathbf{J}_{\parallel}^k)_R. \quad (5.4)$$

Using the two-component uncertainty equation (1.1), this leads to the separability condition for  $S_2$ , the sum of the two-component relative variances:

$$S_2 = \Delta^2 \mathbf{J}_{\parallel}^{total} \geq NC_J, \quad (5.5)$$

If violated, this will imply an entanglement between some of the sites. When three variances are measurable, there are similar conditions known based on three-variance uncertainties.

These relations are useful for identifying the entanglement of maximally entangled states where  $\langle \hat{\mathbf{J}} \rangle = 0$ . For example, the Bell singlet-state  $J = 1/2$  for which the spins are anti-correlated ( $J^{total} = 0$ ) gives the total uncertainty as zero (i.e.,  $S_2 = 0$ ) provided  $c_k = d_k = e_k = 1$ . The many body singlet state in which pairs of particles are in singlet states gives zero total uncertainties for larger  $N$  [49]. Here we consider the maximally entangled states for fixed  $J$  of form (here  $|J, m\rangle$  are the eigenstates of  $J_Z$ )

$$|J, N\rangle_M = \frac{1}{\sqrt{2J+1}} \sum_{m=-J}^J |J, m\rangle^{\otimes N}, \quad (5.6)$$

where spins are correlated. For  $N = 2$ , the sum of the two variances  $\Delta (J_X^A - J_X^B)^2 + \Delta (J_Y^A + J_Y^B)^2$  is always zero, for any  $J$ . Singlet states of total spin zero for  $d$ -level systems have been presented in [50]. We denote the singlet state (which has zero total spin) obtained from  $N$  particles of spin  $J$  as  $|J, N\rangle_S$ .

The two variance sum  $S_2$  is zero for the anti-correlated singlet state. To examine the sensitivity of the two variance criterion to noise, we reduce entanglement by considering the mixed state of the type considered by Werner [51]:

$$\hat{\rho} = p_n \hat{I}_J + (1 - p_n) |J, N\rangle_S \langle J, N|, \quad (5.7)$$

where  $p_n$  gives the relative contribution of the white noise term represented by  $\hat{I}_J = \left[ \hat{I} / (2J + 1) \right]^{\otimes N}$ , which is a rotationally symmetric, uncorrelated state proportional to

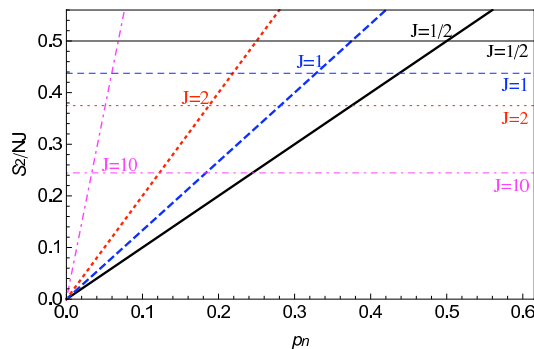


Figure 5. (Color online) Plot of the multipartite entanglement criteria. The sloping, bold lines give the normalized sum of the two spin variances ( $S_2/NJ$ ) for the  $N$  particle singlet state  $|J, N\rangle_S$  mixed with the maximally noisy state, as a function of noise probability  $p_n$ . Entanglement is confirmed when the bold line for each  $J$  falls below the corresponding horizontal line giving  $C_J/J$ . From the bottom, the lines correspond to  $J = 1/2, 1, 2, 10$ .

the identity matrix at each site. Since the singlet state is perfectly correlated, and the Werner state is completely isotropic, one can show that the uncertainties for the multipartite case are entirely due to the white noise terms. From equation (5.5), which requires only two measurement settings, the condition for detecting entanglement is given by:

$$S_2 = \frac{2N}{3} J(J+1) p_n < NC_J. \quad (5.8)$$

which gives the bound of noise for detecting entanglement of:

$$p_n < \frac{3C_J}{2J(J+1)}. \quad (5.9)$$

If all three spin measurements are available, a three spin measurement is even more sensitive to entanglement for this isotropic case. However, in many cases all three components are not measurable, or may not all have strong correlations.

Figure 5 illustrates the purity required in order to demonstrate entanglement between spin  $J$  particles (sites) using the two variance equation (5.5). Entanglement is detected when the normalized two variance sum  $S_2$  is below the line indicating the value of  $C_J/J$ , i.e., when  $S_2/NJ < C_J/J$ .

## VI. OUTLOOK

In conclusion, we have derived an uncertainty relation for the planar sum of the variances in two orthogonal spin directions for systems of fixed total spin. The lower bound varies asymptotically as  $J^{2/3}$ . We have shown that this planar local uncertainty relation can be readily saturated with macroscopic planar squeezed states at large

spin. In addition, a practical technique for generating these states is proposed, employing the ground state of a two-well Bose condensate with attractive interactions.

Such planar squeezed states have the feature that they are able to minimize phase measurement noise over a wide range of unknown phase angles, in an interferometric measurement. Since these states are readily obtainable as ground states of physically relevant Hamiltonians in a two-mode Bose-Einstein condensate, it appears feasible to generate and demonstrate these features in laboratory measurements, either using ground state preparation in an attractive BEC [22], or using dynamical techniques with repulsive interactions.

Criteria for detecting entanglement between multiple spin  $J$  systems using only two component measurements can be derived from this. The two spin component entan-

glement criterion is likely to have important applications where noise or measurement is asymmetric, so that all three components cannot be measured. There are other generalizations possible if one constrains  $\langle \hat{J}_Z \rangle$  to have a finite value, giving an inequality involving  $C_J(\bar{J}_Z)$ ; these will be treated elsewhere. We expect similar relations to occur for other continuous groups.

## ACKNOWLEDGMENTS

We wish to thank the Humboldt Foundation, Heidelberg University, and the Australian Research Council for funding via AQUAO COE and Discovery grants, as well as useful discussions with Markus Oberthaler, Philip Treutlein and Andrei Sidorov.

- 
- [1] M. Kitagawa and M. Ueda, *Phys. Rev. A* **47**, 5138 (1993).  
 [2] D. J. Wineland, J. Bollinger, W. M. Itano, and D. J. Heinzen, *Phys. Rev. A* **50**, 67 (1994).  
 [3] J. Estève, C. Gross, A. Weller, S. Giovanazzi, M. K. Oberthaler, *Nature* **455**, 1216 (2008).  
 [4] C. Gross, T. Zibold, E. Nicklas, J. Esteve, and M. K. Oberthaler, *Nature* **464**, 1165 (2010).  
 [5] M. F. Riedel, P. Bhi, Y. Li, T. W. Haensch, A. Sinatra, and Philipp Treutlein, *Nature* **464**, 1170 (2010).  
 [6] V. Vedral, *Nature* **453**, 1004 (2008).  
 [7] H. F. Hofmann and S. Takeuchi, *Phys. Rev. A* **68**, 032103 (2003).  
 [8] G. Toth, C. Knapp, O. Guhne, and H. Briegel, *Phys. Rev. Lett.* **99**, 250405 (2007).  
 [9] G. Toth, C. Knapp, O. Guhne, and H. Briegel, *Phys. Rev. A* **79**, 042334 (2009).  
 [10] E. G. Cavalcanti, P. D. Drummond, H. A. Bachor and M. D. Reid, *Optics Express* **17**, 18693 (2009).  
 [11] H. M. Wiseman, S. J. Jones, and A. C. Doherty, *Phys. Rev. Lett.* **98**, 140402 (2007).  
 [12] S. J. Jones, H. M. Wiseman, and A. C. Doherty, *Phys. Rev. A* **76**, 052116 (2007).  
 [13] E. G. Cavalcanti, S. J. Jones, H. M. Wiseman, and M. D. Reid, *Phys. Rev. A* **80**, 032112 (2009).  
 [14] D. J. Saunders, S. J. Jones, H. M. Wiseman and G. J. Pryde, *Nature Physics* **6**, 845 (2010).  
 [15] R. W. Finkel, *Phys. Rev. A* **35**, 1486 (1987).  
 [16] N. Kiesel, C. Schmid, G. Toth, E. Solano, and H. Weinfurter, *Phys. Rev. Lett.* **98**, 063604 (2007).  
 [17] G. Toth, *J. Opt. Soc. Am. B* **24**, 275 (2007).  
 [18] See: <http://reference.wolfram.com/mathematica/ref/FindMinimum.html>.  
 [19] C. Aragone, G. Guerri, S. Salamo, and J. L. Tani, *J. Phys. A* **7**, L149 (1974).  
 [20] J. I. Cirac, M. Lewenstein, K. Molmer, and P. Zoller, *Phys. Rev. A* **57**, 1208 (1998).  
 [21] L. D. Carr, D. R. Dounas-Frazer, and M. A. Garcia-March, *EPL* **90**, 10005 (2010).  
 [22] Q. Y. He, M. D. Reid, C. Gross, M. Oberthaler, P. D. Drummond, *Phys. Rev. Lett.* **106**, 120405 (2011).  
 [23] Andrew P. Hines, Ross H. McKenzie, and Gerard J. Milburn, *Phys. Rev. A* **67**, 013609 (2003).  
 [24] Q. Xie, Q. and W. Hai, *Eur. Phys. J. D* **39**, 277 (2006).  
 [25] A. J. Ferris, M. K. Olsen, E. G. Cavalcanti and M. J. Davis, *Physical Review A* **78**, 060104 (2008).  
 [26] D. W. Hallwood, Thomas Ernst and Joachim Brand, *Phys. Rev. A* **82**, 063623 (2010).  
 [27] N. Bar-Gill, C. Gross, I. Mazets, M. Oberthaler, and G. Kurizki, *Phys. Rev. Lett.* **106**, 120404 (2011).  
 [28] M. Fattori, C. D'Errico, G. Roati, M. Zaccanti, M. Jona-Lasinio, M. Modugno, M. Inguscio, and G. Modugno, *Phys. Rev. Lett.* **100**, 080405 (2008).  
 [29] M. Vengalattore, J. M. Higbie, S. R. Leslie, J. Guzman, L. E. Sadler, and D. M. Stamper-Kurn, *Phys. Rev. Lett.* **98**, 200801 (2007).  
 [30] Holger Müller, Sheng-wei Chiow, Quan Long, Sven Herrmann, and Steven Chu, *Phys. Rev. Lett.* **100**, 180405 (2008).  
 [31] J. E. Debs, P. A. Altin, T. H. Barter, D. Doring, G. R. Dennis, G. McDonald, N. P. Robins, and J. D. Close, arXiv:1011.5804v2.  
 [32] A. D. Cronin, J. Schmiedmayer, and D. E. Pritchard, *Rev. Mod. Phys.* **81**, 1051-1129 (2009).  
 [33] R. P. Anderson, C. Ticknor, A. I. Sidorov, and B. V. Hall, *Phys. Rev. A* **80**, 023603 (2009).  
 [34] M. D. Reid, *Phys. Rev. A* **40**, 913 (1989).  
 [35] M. D. Reid, *et al.*, *Rev. Mod. Phys.* **81**, 1727-1751 (2009).  
 [36] L. Duan, G. Giedke, J. I. Cirac and P. Zoller, *Phys. Rev. Lett.* **84**, 2722-2725 (2000).  
 [37] V. Giovannetti, S. Mancini, D. Vitali and P. Tombesi, *Phys. Rev. A* **67**, 022320 (2003).  
 [38] K. Dechoum, S. Chaturvedi, P. D. Drummond, and M. D. Reid, *Phys. Rev. A* **70**, 053807 (2004).  
 [39] A. Sørensen, L.-M. Duan, J. I. Cirac and P. Zoller, *Nature* **409**, 63-66 (2001).  
 [40] G. Toth, *Phys. Rev. A* **69**, 052327 (2004).  
 [41] M. Wiesniak, V. Vedral and C. Brukner, *New Journ. Phys.* **7**, 258 (2005).  
 [42] J. K. Korbicz, J. I. Cirac and M. Lewenstein, *Phys. Rev. Lett.* **95**, 120502 (2005).  
 [43] S. B. Papp *et al.*, *Science* **324**, 764-768 (2009).  
 [44] A. S. Sørensen and K. Mølmer, *Phys. Rev. Lett.* **86**, 4431 (2001).  
 [45] E. G. Cavalcanti and M. D. Reid, *Journ. Mod. Opt.* **54**, 2373 (2007);

- [46] E. G. Cavalcanti and M. D. Reid, Phys. Rev. Lett. **97**, 170405 (2006).
- [47] J. S. Bell, Physics **1**, 195 (1964).
- [48] J. F. Clauser, M. A. Horne, A. Shimony and R. A. Holt, Phys. Rev. Lett. **23**, 880 (1969).
- [49] G. Toth and M. Mitchell, New Journ. Phys. **12**, 053007 (2010).
- [50] A. Cabello, Journ. Mod. Opt. **50**, 1049 (2003).
- [51] R. F. Werner, Phys. Rev. A **40**, 4277 (1989).